PERIODICA POLYTECHNICA SER. CIV. ENG. VOL. 46, NO. 1, PP. 115–124 (2002)

LONGITUDINAL BEHAVIOUR OF RAIL EMBEDDED IN ELASTIC MATERIAL

Gyula KORMOS

Department of Highway and Railway Engineering
Budapest University of Technology and Economics
H–1521 Budapest, Hungary

Received: March 30, 2001

Abstract

The longitudinal behaviour of a rail embedded in elastic material is different from that laid on ballast track, studied in the professional literature. The longitudinal coefficient of elasticity of the built in elastic embedding material could be determined unambiguously only by testing. On that basis the dilatation behaviour of a rail can be represented by a discrete model allowing to determine the internal forces raised in the rail and the displacement of its cross sections as well as the length of the moving section.

Keywords: dilatation, displacement of the moving section, continuously embedded rail systems.

1. Introduction

Embedding of a rail laid in an elastic material poured into a concrete or steel recess gives to it continuous flexible support and lateral fixing. The calculation of the strains of these supports is similar to that related to the ballast track in several aspects. In case the longitudinal behaviour of the rail is under scrutiny, however, substantial differences have to be expected.

Although the behaviour of the ballast track is more or less known from the professional literature [2, 6, 7, 10], an approximation made in the calculations has to be mentioned. As the tests approved, actually the longitudinal resistance of the ballast track is developing gradually (see *Fig. 1*). Following a displacement of some millimeters the longitudinal resistance reaches its maximum and that value does not change any more during further displacement [7, 10]. Aiming to facilitate practical calculations, the initial section with changing resistance is traditionally neglected, i.e. only a constant value (see *Fig. 2*) is taken into account.[1] Thus along with the increase of temperature, the distribution of internal forces will be linear from the fish-plated, or free end of the rail up to the full value of the dilatation force [2, 6, 7, 10]. The displacement of the K cross section on the moving section is proportional with the measured value of the T 'force-area' (*Fig.3*).

[1] For exact calculations dilatational behaviour should be described by differential equations and the final formulae include hyperbolic functions.

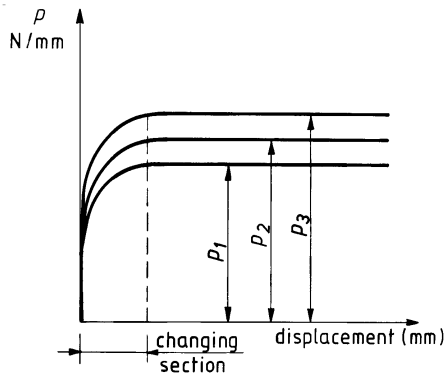

Fig. 1. Longitudinal resistance of various ballast tracks

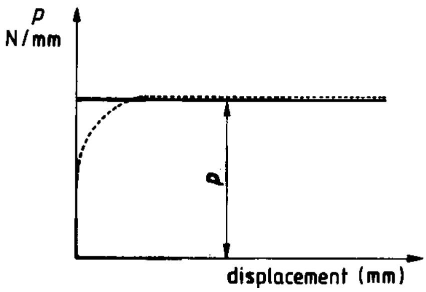

Fig. 2. Assumption of constant longitudinal resistance

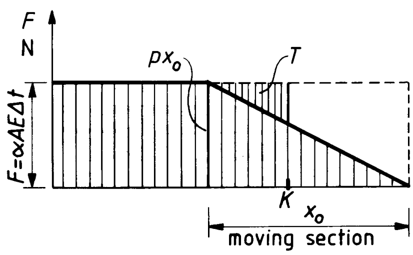

Fig. 3. Normal forces raising in a welded track's rail laid on ballast

In case of a rail embedded in an elastic embedding material, this latter could bear longitudinal displacements until these cause damages on the long term [3, 4]. It means, the embedding material is able to support and fix the superstructure when on the one hand the maximum dilatation force causes less displacement of the rail's end than that damaging the embedding material or its superficial coating and provides appropriately flexible embedding in all spatial directions.

It is obvious that when determining the longitudinal strains of an elastically embedded rail – differently from methodology applied for ballast track –, only the elastic domain of the embedding material's displacement could be taken into account. Since under the impact of the dilatation force the displacement of each cross section on the moving section reaches that of the rail's end gradually, it is commonplace that the embedding material's longitudinal resistance is also changing gradually, proportionally with the displacement. Taking into consideration, that neither the distribution of the internal forces, nor the displacements of the moving section are known previously, determining the longitudinal behaviour of a rail embedded in an elastic material is much more complicated than that laid on ballast track [4].

2. Determining the Longitudinal Resistance of the Elastic Bedding Material

The longitudinal resistance features of an elastic bedding material can be determined in theory, but the width of the bedding material placed between the rail's cross section and the space filling elements (put in to reduce the volume of the bedding material) is varying, therefore the internal spatial displacements of the elastic bedding material are extremely different from each other. Instead of the sophisticated calculations incorporated into the highly uncertain model, the determination of the longitudinal resistance by testing offers a much easier way [4, 5] to follow.

As a consequence of the bedding material's elasticity, the longitudinal resistance increases proportionally with the rail's displacement. This longitudinal change of resistance could be characterised by the coefficient of elasticity. This can be determined by testing, e.g. moving a rail (*Fig. 4*) embedded in a short ($l = 1.00$ m) recess, and recording the co-ordinates of a force-displacement (F, u) diagram. It is worthwhile to repeat the test several times, during the preparation of the proofbar, as well as during and after the charging cycle in that domain of the displacements, where the bedding material remains completely elastic [1, 8, 9]. Finally, following a series of measurements, the rail should be moved until the embedding of the proofbar collapses [4, 5]. The completely elastic domain of the displacements, the start and the development of the collapse may be well perceived from the force-displacement diagrams (*Fig. 5*). When implementing serial measurements it has to be taken into consideration, that bedding materials have often dumping effects, therefore the series of charges and discharges must be separated by appropriate waiting times.

The *longitudinal coefficient of elasticity* is the steepness:

$$\rho \ [\mathrm{N/mm^2}]$$

of the force-displacement diagram related to the completely elastic domain. For

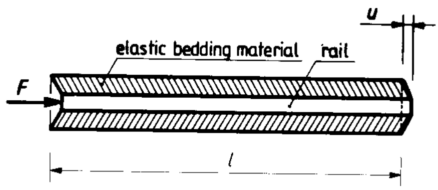

Fig. 4. Deformation of elastic material during a push test

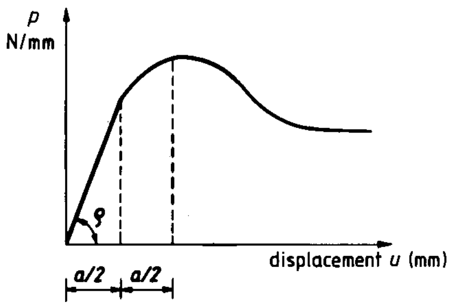

Fig. 5. Longitudinal resistance of elastic material

practical reasons it is more suitable to characterise it by a different dimension:

$$\rho \text{ [N/mm/m]}$$

since it reflects clearly, how many kN force is needed to displace the end of a 1.00 m long proofbar-rail by 1 mm. The transformation of the measurements' results obtained with proofbar-rails of various length becomes less ambiguous as well.

The bedding material under scrutiny is considered acceptable, when the maximum dilatation displacement of the rail's end, calculated on the base of the minimum longitudinal coefficient of elasticity obtained during the serial charging tests (*Fig.*6) does never exceed the upper limit value of the elastic domain of the displacements [3, 4], and at the same time it has got the required support and fixing characteristics. During actual measurements the upper limit value of the displacement related to the elastic domain is generally half of that value related to the start of the collapse (*Fig.* 5).

3. Dilatational Behaviour of a Rail Embedded in a Flexible Material

The deformation of the bedding material caused by the dilatation movement of a rail embedded in an elastic material (*Fig.* 7) appears gradually, starting from the middle

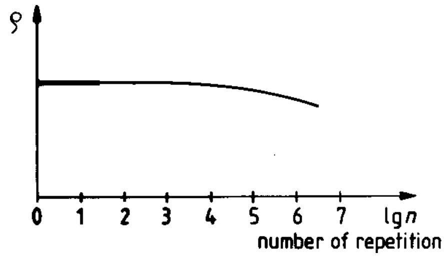

Fig. 6. Changes of the elastic material's longitudinal coefficient of elasticity under the impact of repeated charges

cross section, while this cannot be perceived due to the shortness of the proofbar-rail (*Fig. 4*). Since neither the distribution of the internal forces, nor the rail's movement is known beforehand, these parameters cannot be determined directly. Nevertheless, it is well known that the retaining force appearing in the bedding material is directly proportional with the displacement of the rail and in the middle of the rail length L a dilatation force of

$$F_{\mathrm{dil}} = \alpha \cdot AE \cdot \Delta t \tag{1}$$

appears, where

α	$^\circ\mathrm{C}^{-1}$	the coefficient of linear heat-expansion of the rail's steel,
A	mm^2	the area of the rail's cross section,
E	$\mathrm{N/mm}^2$	the coefficient of flexibility of the rail's steel,
Δt	$^\circ\mathrm{C}$	the variations of temperature.

Aiming to determine the dilatation behaviour of an L m long (*Fig. 7*) superstructure, it seems to be appropriate to apply a discrete model [1, 3, 8, 9]. For that purpose, starting from the middle of the superstructure, the rail's length has to be divided with appropriate density into n pieces of l long sections, while the retaining force of the bedding material is represented on each section by a sole spring characterised by a spring constant of $\rho \cdot l$, assuming that the spring force is acting at the end of the l long sections (*Fig. 8*). In that way the state of equilibrium of n 'nodes' can be studied. Taking into consideration, however, that the distribution of the internal forces is unknown, let us charge the ends of the rail with a force F equal to the dilatation force according to (1). In that case a normal force of $F = F_{\mathrm{dil}}$ will appear all along the rail, therefore none of its cross sections can be displaced. (This state of equilibrium is equivalent to that when the movement of both ends of the rail is prevented before the temperature is changing.)

In that state of equilibrium the 'nodes' are charged with displacements u_1, u_2, $\ldots$, u_i, $\ldots$, u_{n-1}, u_n when

$$u_1 < u_2 < \ldots < u_i < u_{n-1} < u_n \tag{2}$$

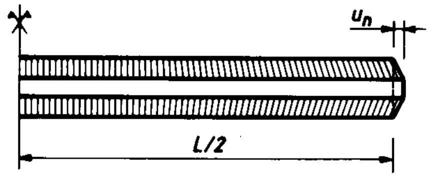

Fig. 7. Deformation of elastic bedding material under the impact of dilatation movement of a superstructure with free rail's end

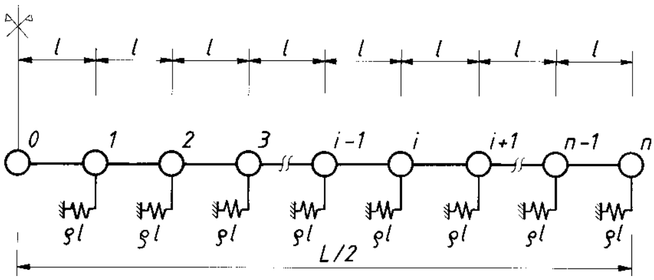

Fig. 8. Formulation of a discrete model

(see *Fig. 9*), and equilibrium equations can be formulated for each node on the base of *Fig. 10*. (The positive directions of the equilibrium equations' forces and displacements are also marked in the figure).

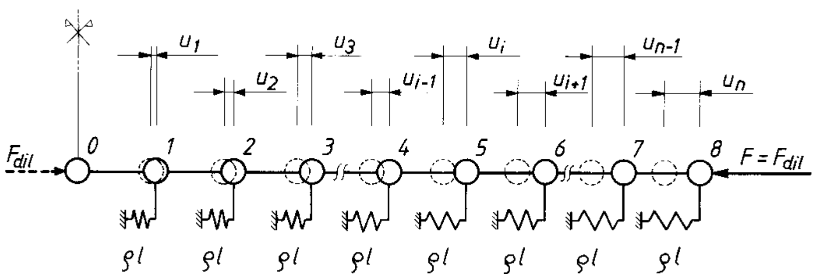

Fig. 9. Charging the nodes of the discrete model with displacements

According to the Hooke law:

$$\sigma = E \cdot \varepsilon \tag{3}$$

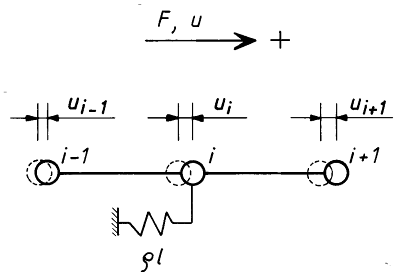

Fig. 10. Study of node N° i

an ε specific extension of an elastic material (the rail) generates σ tension in the rail, therefore, in line with *Eq.* (3) the force needed to create an expected u_i displacement can be determined by the following equation:

$$F_i = \frac{EA}{l} u_i. \tag{4}$$

The retaining impact of the flexible material can be calculated as follows:

$$\rho \cdot l \cdot u_i. \tag{5}$$

On the basis of *Fig. 10* and using *Eqs.* (4) and (5), the following equilibrium equation related to node i can be formulated [1, 3, 4, 8]:

$$-\frac{EA}{l}(u_i - u_{i-1}) + \frac{EA}{l}(u_{i+1} - u_i) - \rho \cdot l \cdot u_i = 0, \tag{6}$$

which can be transformed as follows:

$$\frac{EA}{l} u_{i-1} - \left(\frac{2EA}{l} + \rho \cdot l\right) u_i + \frac{EA}{l} u_{i+1} = 0. \tag{7}$$

This equation is valid for the node No. 1 too. Knowing, however, that $u_0 = 0$, in case of node No. 1 instead of (7) the following equation will reflect the state of equilibrium:

$$-\left(\frac{2EA}{l} + \rho \cdot l\right) u_1 + \frac{EA}{l} u_2 = 0. \tag{8}$$

The case of node n is slightly different, because at the end of the rail there is a support equal to the dilatation force F_{dil}, therefore the state of equilibrium is represented by the following equation:

$$\frac{EA}{l} u_{n-1} - \left(\frac{EA}{l} + \rho \cdot l\right) u_n - F_{\text{dil}} = 0. \tag{9}$$

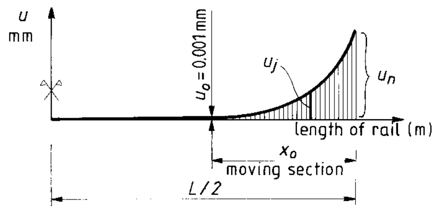

Fig. 11. Dilatation displacements of rail's cross sections embedded in elastic material

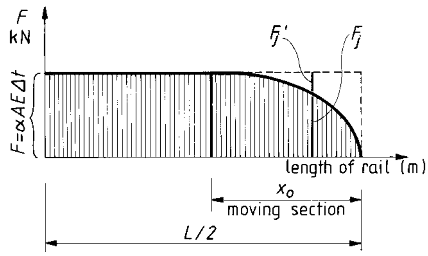

Fig. 12. Normal forces raising in a rail embedded in elastic material and caused by changing temperature

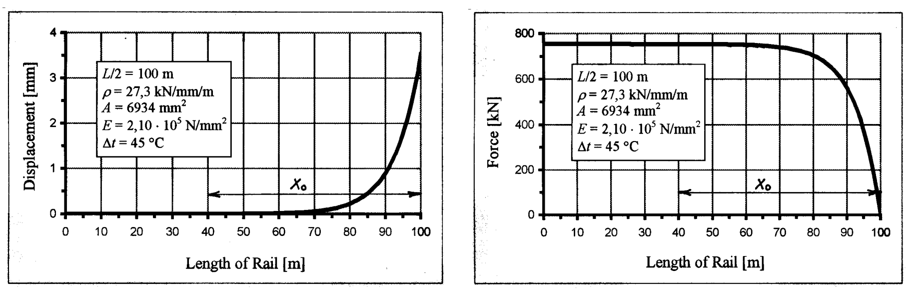

Fig. 13. Force-displacement diagrams of a rail type UIC 54

(It has to be noted that the coefficient in the middle term of the equation's left side above is different from that $2EA$ used previously).

Relating to the nodes altogether n equations can be formulated, where the number of unknown displacement is also n, therefore the system of equations can be solved. After the replacement of the following coefficients:

$$\frac{EA}{l} = B, \quad -\left(\frac{2EA}{l} + \rho \cdot l\right) = C \quad \text{and} \quad -\left(\frac{EA}{l} + \rho \cdot l\right) = D. \tag{10}$$

Taking into consideration the statements (7), (8), (9) and (10) the system of equations can be formulated as follows [1, 3, 4, 8]:

$$\begin{bmatrix} C & B & & & & & & & & \\ B & C & B & & & & & & & \\ & B & C & B & & & & & & \\ & & B & C & B & & & & & \\ & & & \ddots & \ddots & \ddots & & & & \\ & & & & \ddots & \ddots & \ddots & & & \\ & & & & & \ddots & \ddots & \ddots & & \\ & & & & & & B & C & B & \\ & & & & & & & B & C & B \\ & & & & & & & & B & D \end{bmatrix} \cdot \begin{bmatrix} u_1 \\ u_2 \\ u_3 \\ \vdots \\ \vdots \\ u_i \\ \vdots \\ \vdots \\ u_{n-1} \\ u_n \end{bmatrix} + \begin{bmatrix} 0 \\ 0 \\ 0 \\ \vdots \\ \vdots \\ 0 \\ \vdots \\ \vdots \\ 0 \\ -F_{\mathrm{dil}} \end{bmatrix} = \begin{bmatrix} 0 \\ 0 \\ 0 \\ \vdots \\ \vdots \\ 0 \\ \vdots \\ \vdots \\ 0 \\ 0 \end{bmatrix} \tag{11}$$

or using simpler symbols:

$$\underline{\underline{\mathbf{A}}} \cdot \underline{\mathbf{u}} + \underline{\mathbf{F}} = \underline{\mathbf{0}}. \tag{12}$$

The displacements of given cross sections of the rail ('nodes') can be determined [3, 4] by solving (12), i. e. using

$$\underline{\mathbf{u}} = -\underline{\underline{\mathbf{A}}}^{-1} \cdot \underline{\mathbf{F}}. \tag{13}$$

Taking into consideration that the retaining impact of an l long elastic embedding material reflects the change of normal force on the l long section lying between two neighbouring nodes, the distribution of normal forces can be calculated (*Fig. 12*) using formulae (1) and (5) as well as u displacements derived from (13) in the following equation [4]:

$$F_j = F_{\mathrm{dil}} - F'_j = F_{\mathrm{dil}} - \rho \cdot l \cdot \sum_{i=1}^{j} u_i. \tag{14}$$

In mathematical sense the u_i displacements are varying all along the L long superstructure, except the middle cross section, which do not move in theory. During actual calculations it can be observed, however, that at a given superstructure the last section of the displacements presents exactly the same features. In case when a displacement smaller than $u_0 = 0.001$ mm is not considered to be an actual movement, according to *Fig. 11*, the x_0 length of the moving section is unambiguously determined by the u_0 limit value of the displacement. The length of the moving section for a given superstructure will always be the same. It can be stated therefore, that *the behaviour of a rail embedded into elastic material is practically identical to that of a welded track* [3, 4].

Fig. 13 presents diagrams of displacements and internal forces related to a rail type UIC 54 embedded into an elastic material characterised by a longitudinal coefficient of elasticity of $\rho = 27.3$ kN/mm/m, built with an $L/2 = 100$ m half-length.

References

[1] Theoretical and Laboratory Studies Needed for Eligibility Certificate of Edilon Type Superstructure. Summarization Report, BME: 14746 (234.004/95.) Budapest, 1996, pp. 111–152, 202–230.

[2] KLUGAR, K., Eisenbahn- und Verkehrswesen I. Technische Universität Graz, 1977, pp. 208–214.

[3] KORMOS, GY., Welded Railway Superstructure, Record, manuscript, pp. 4–14.

[4] KORMOS, GY., The Longitudinal Behaviour of the Rail Embedded in Flexible Material, *Közlekedéstudományi Szemle*, **LI/10** (2001), pp. 364–369.

[5] LUDVIGH, E., Elastic Behaviour of Continuously Embedded Rail Systems, *Periodica Polytechnica*, **1** (2001) (under publishing).

[6] MEGYERI, J., *Railway Engineering*, Műegyetemi Kiadó, Budapest, 1997, pp. 185–194.

[7] NEMESDY, E., *Railway Superstructure*, Tankönyvkiadó, Budapest, 1966, pp. 242–313.

[8] Study of Edilon Type 54 Rail System Concrete Recess Railway Superstructure Used on Railway Bridges, 1st report, BME: 20503, Budapest, 1996, pp. 21–37, 64–105.

[9] Study of Edilon Type 54 Rail System Steel Recess Railway Superstructure Used on Railway Bridges, 2nd report, BME: 20503, Budapest, 1997, pp. 11–34, 64–150.

[10] VÁSÁRHELYI, B. (ed.), *Welded Railway Tracks*, Műszaki Könyvkiadó, Budapest, 1960, pp. 182–245.